LETTER

doi:10.1038/nature10400

Caspase-8 regulates TNF-α-induced epithelial necroptosis and terminal ileitis

Claudia Günther[1], Eva Martini[1], Nadine Wittkopf[1], Kerstin Amann[2], Benno Weigmann[1], Helmut Neumann[1], Maximilian J. Waldner[1], Stephen M. Hedrick[3], Stefan Tenzer[4], Markus F. Neurath[1] & Christoph Becker[1]

Dysfunction of the intestinal epithelium is believed to result in the excessive translocation of commensal bacteria into the bowel wall that drives chronic mucosal inflammation in Crohn's disease, an incurable inflammatory bowel disease in humans characterized by inflammation of the terminal ileum[1]. In healthy individuals, the intestinal epithelium maintains a physical barrier, established by the tight contact of cells. Moreover, specialized epithelial cells such as Paneth cells and goblet cells provide innate immune defence functions by secreting mucus and antimicrobial peptides, which hamper access and survival of bacteria adjacent to the epithelium[2]. Epithelial cell death is a hallmark of intestinal inflammation and has been discussed as a possible pathogenic mechanism driving Crohn's disease in humans[3]. However, the regulation of epithelial cell death and its role in intestinal homeostasis remain poorly understood. Here we demonstrate a critical role for caspase-8 in regulating necroptosis of intestinal epithelial cells (IECs) and terminal ileitis. Mice with a conditional deletion of caspase-8 in the intestinal epithelium (*Casp8*$^{\Delta IEC}$) spontaneously developed inflammatory lesions in the terminal ileum and were highly susceptible to colitis. *Casp8*$^{\Delta IEC}$ mice lacked Paneth cells and showed reduced numbers of goblet cells, indicating dysregulated antimicrobial immune cell functions of the intestinal epithelium. *Casp8*$^{\Delta IEC}$ mice showed increased cell death in the Paneth cell area of small intestinal crypts. Epithelial cell death was induced by tumour necrosis factor (TNF)-α, was associated with increased expression of receptor-interacting protein 3 (*Rip3*; also known as *Ripk3*) and could be inhibited on blockade of necroptosis. Lastly, we identified high levels of RIP3 in human Paneth cells and increased necroptosis in the terminal ileum of patients with Crohn's disease, suggesting a potential role of necroptosis in the pathogenesis of this disease. Together, our data demonstrate a critical function of caspase-8 in regulating intestinal homeostasis and in protecting IECs from TNF-α-induced necroptotic cell death.

Caspase-8 is a cysteine protease critically involved in regulating cellular apoptosis. On activation of death receptors, including TNF-receptor and Fas, caspase-8 is activated by limited autoproteolysis and the processed caspase-8 subsequently triggers the caspase cascade that finally leads to apoptotic cell death. Caspase-mediated apoptosis is important for the turnover of IECs and for shaping the morphology of the gastrointestinal tract[4]. Furthermore, recent data have indicated a role of caspase-mediated apoptosis of IECs in the pathogenesis of inflammatory bowel diseases (IBDs) such as Crohn's disease and ulcerative colitis[5,6].

To study the function of caspase-8 in the gut, we generated mice with an IEC-specific deletion of caspase-8 (*Casp8*$^{\Delta IEC}$). Accordingly, mice with floxed caspase-8 alleles were bred with mice expressing the Cre recombinase under the control of the IEC-specific villin promoter. Specific deletion of caspase-8 in IECs was confirmed by polymerase chain reaction (PCR) and western blotting (Supplementary Fig. 1a, b). *Casp8*$^{\Delta IEC}$ mice were born at the expected Mendelian ratios and developed normally, although weighing on average slightly less than control littermates at 8 weeks of age (data not shown). Despite the paradigm that apoptosis is important for regulating epithelial cell numbers[4], histological and morphometrical analysis of the jejunum and colon of *Casp8*$^{\Delta IEC}$ mice showed no overt changes of tissue architecture or dysregulation of apoptosis (Supplementary Figs 1d–f and 2). Although this suggested that caspase-8 is not essential for the structural development of the gut, high-resolution endoscopy showed erosions in the terminal ileum—but not in the colon—of *Casp8*$^{\Delta IEC}$ mice (Fig. 1a and Supplementary Fig. 1c). Histological analysis demonstrated marked destruction of the architecture and signs of inflammation including bowel wall thickening, crypt loss and increased cellularity in the lamina propria (Fig. 1b) in more than 80% of all ileal specimens. This finding of spontaneous ileitis in the absence of caspase-8 in IECs was further supported by increased expression of the inflammation markers *S100a9* and *TNF-α* (also known as *Tnf*) and by elevated infiltration of the lamina propria with CD4$^+$ T cells and granulocytes (Fig. 1c and Supplementary Fig. 3).

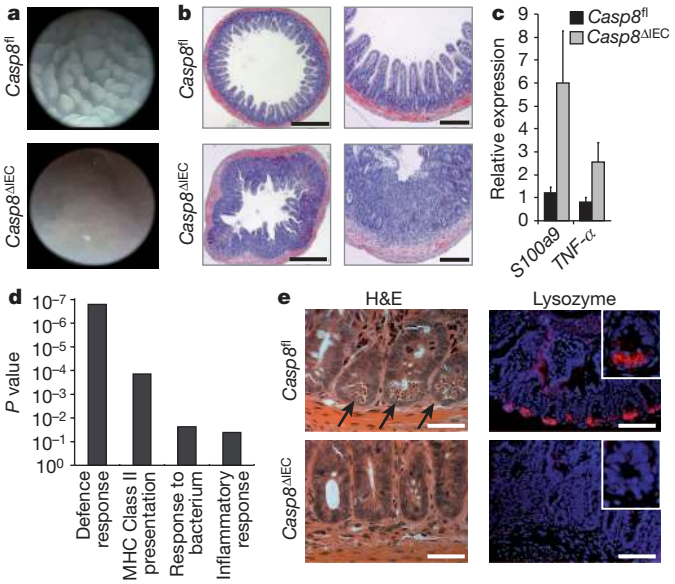

Figure 1 | *Casp8*$^{\Delta IEC}$ mice spontaneously develop ileitis and lack Paneth cells. **a**, **b**, Representative endoscopic pictures (**a**) and H&E stained cross-sections (**b**) showing villous erosions in the terminal ileum of *Casp8*$^{\Delta IEC}$. Scale bars, 500 μm (left), 200 μm (right). **c**, RT–PCR showing increased level of inflammatory markers in the terminal ileum of *Casp8*$^{\Delta IEC}$ mice (6 mice per group + s.e.m., relative to *Hprt*). **d**, GO analysis of genes significantly downregulated in gene-chip analysis of IECs from three control and three *Casp8*$^{\Delta IEC}$ mice. **e**, Ileum cross-sections stained with H&E (scale bars, 50 μm) and lysozyme (scale bars, 100 μm) for Paneth cells (inset shows single crypt at higher magnification). Arrows indicate crypt bottom with Paneth cells.

[1]Department of Medicine 1, Friedrich-Alexander-University, D-91054 Erlangen, Germany. [2]Department of Nephropathology, Friedrich-Alexander-University, D-91054 Erlangen, Germany. [3]Department of Cellular and Molecular Medicine, University of California, San Diego, La Jolla, California 92093, USA. [4]Institute of Immunology, Johannes Gutenberg University, D-55131 Mainz, Germany.

To investigate whether caspase-8 deficiency sensitizes mice to experimental intestinal inflammation in the large intestine, we subjected *Casp8*$^{\Delta IEC}$ and control mice to dextran sodium sulphate, a well-established model of experimental colitis. Notably, we observed high lethality in the group of *Casp8*$^{\Delta IEC}$ mice but not in control mice (Supplementary Fig. 4). Moreover, the former lost significantly more weight than controls. All *Casp8*$^{\Delta IEC}$ but none of the control mice developed rectal bleeding and endoscopic and histological signs of very severe colitis with epithelial erosions, a finding that was confirmed by quantitative PCR for the IEC marker villin. Together, our data indicate that a lack of caspase-8 in IECs renders mice highly susceptible to spontaneous ileitis and experimentally induced colitis.

To screen for molecular mechanisms that sensitize *Casp8*$^{\Delta IEC}$ mice for intestinal inflammation, we next performed whole-genome gene-chip analysis of IECs from unchallenged control and *Casp8*$^{\Delta IEC}$ mice. Of the 45,000 expression tags analysed, 197 were significantly downregulated and 136 upregulated in *Casp8*$^{\Delta IEC}$ mice (fold change >2.0, $P < 0.05$) (Supplementary Table 1). Gene ontology (GO) analysis of downregulated genes showed that several biological pathways were impaired in *Casp8*$^{\Delta IEC}$ mice as compared to littermate controls, with the GO terms "defence response" and "MHC class II antigen presentation" reaching very high levels of significance (Fig. 1d). Within the group of genes upregulated in *Casp8*$^{\Delta IEC}$ mice, no GO term reached significance levels. Notably, within the defence response gene set, genes belonging to the family of antimicrobial peptides including several defensins, lysozyme and phospholipases were among the most strongly downregulated genes (Supplementary Fig. 5a), suggesting defects in the antimicrobial defence of the intestinal epithelium in the absence of epithelial caspase-8. Expression of antimicrobial peptides is a hallmark of Paneth cells, epithelial-derived cells that are located at the base of the crypts of Lieberkuehn in the small intestine[7]. Within Paneth cells, antimicrobial peptides are stored in cytoplasmatic granules, from which they can be released into the gut lumen, thereby contributing to intestinal host defences. Notably, *Casp8*$^{\Delta IEC}$ mice showed a complete absence of cells with secretory granules and lysozyme expression at the crypt base of the small intestine, suggesting that Paneth cells are lacking in the gut of these animals (Fig. 1e). Furthermore, the number of mucus-secreting goblet cells was reduced, as indicated by staining with ulex europaeus agglutinin 1 (UEA-1), a lectin binding to glycoproteins characteristic for these cells (Supplementary Fig. 5b). In contrast, we observed no changes in the appearance of enteroendocrine cells or absorptive enterocytes, as indicated by staining for chromogranin-A or alkaline phosphatase, respectively (Supplementary Fig. 5b). The lack of Paneth cells and partial lack of goblet cells was confirmed by quantitative gene expression analysis showing diminished expression of Paneth-cell- and goblet-cell-specific genes, whereas expression of genes specific for enteroendocrine cells, enterocytes and progenitor cells was unchanged (Supplementary Fig. 5c). Thus, collectively, our data indicate that deficient expression of caspase-8 in the intestinal epithelium results in diminished Paneth and goblet cell numbers and hence may lead to defects in antimicrobial host defence and terminal ileitis.

In addition to controlling apoptosis, there is growing evidence that caspase-8 regulates several non-apoptotic cellular mechanisms including proliferation, migration and differentiation[8,9]. Accordingly, caspase-8 has been shown to promote the terminal differentiation of macrophages and keratinocytes[10]. Thus, we reasoned that caspase-8 might support intestinal immune homeostasis by promoting the terminal differentiation of Paneth and goblet cells. To verify this hypothesis, we performed long-term organoid cultures of small intestinal crypts *in vitro* as previously described[11]. Isolated crypts from the small intestine underwent multiple crypt fissions forming large organoids in both control and *Casp8*$^{\Delta IEC}$ mice (Supplementary Fig. 6a). In marked contrast to the absence of Paneth cells in crypts from *Casp8*$^{\Delta IEC}$ mice *in vivo*, organoids grown from these crypts *in vitro* over a period of 1–4 weeks showed Paneth cells indistinguishable in localization and number from organoids cultured from control littermate mice (Fig. 2a).

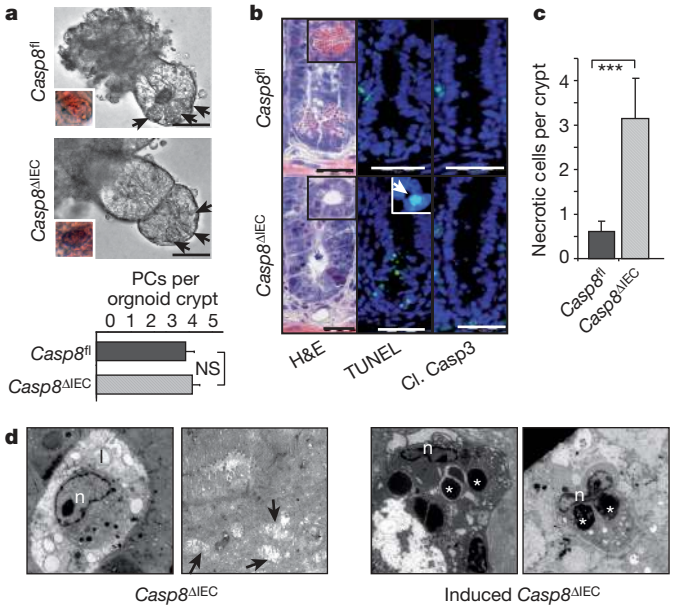

Figure 2 | Increased caspase-8-independent cell death within crypts of *Casp8*$^{\Delta IEC}$ mice. **a**, Representative pictures of gut organoids (scale bars, 50 μm) Arrows indicate Paneth cells. Insets show eosin staining indicating Paneth cells. Graph show number of Paneth cells (PCs) per organoid crypt ($n = 24$) + s.e.m. NS, not significant. **b**, Crypt cross-sections from the small intestine of control and *Casp8*$^{\Delta IEC}$ mice stained with H&E (scale bars, 20 μm), TUNEL (inset shows condensed nuclei) and cleaved caspase-3 (Cl. Casp3) (scale bars, 50 μm). **c**, Quantification of necrotic cells per crypt + s.d. of control ($n = 9$) and *Casp8*$^{\Delta IEC}$ ($n = 14$) mice. **d**, Electron microscopic pictures of dying crypt cells in *Casp8*$^{\Delta IEC}$ mice and inducible *Casp8*$^{\Delta IEC}$. Asterisks indicate Paneth cell granules; arrows indicate mitochondrial swelling. l, crypt lumen; n, nuclei.

PCR analysis confirmed deletion of the caspase-8 allele in Paneth-cell-positive organoids derived from *Casp8*$^{\Delta IEC}$ mice (Supplementary Fig. 6b). Thus, our data indicate that caspase-8 is not required for the differentiation of IECs into Paneth cells, but that a factor present *in vivo* either inhibited the development of or ablated Paneth cells in the absence of caspase-8 expression.

Indeed, *Casp8*$^{\Delta IEC}$ mice showed a large number of dying epithelial cells at the crypt base with pyknotic nuclei and a shrunken eosinophilic cytoplasm (Fig. 2b), implying that caspase-8-deficient Paneth and goblet cells might be sensitive to cell death. Dying crypt cells usually lacked typical apoptotic body formation, suggesting necrotic rather than apoptotic cell death. This conclusion was supported by the observation that dying cells were TdT-mediated dUTP nick end labelling (TUNEL) positive, but showed no activation of caspase-3 (Fig. 2b). The number of necrotic cells at the crypt base was significantly higher in *Casp8*$^{\Delta IEC}$ mice as compared to control mice (Fig. 2c). Lastly, electron microscopy of the crypt area demonstrated cells with typical features of necrosis including mitochondrial swelling and extensive vacuole formation while typically lacking the blebbing usually associated with apoptosis (Fig. 2d). Importantly, many cells with features of necrosis also showed electron-dense granules, indicating necrotic Paneth cells. This conclusion was supported by electron microscopy of mice in which the caspase-8 deletion was induced in adult mice by injection with tamoxifen (inducible *Casp8*$^{\Delta IEC}$) to detect early effects of caspase-8 deletion. Taken together, our data indicate that the lack of caspase-8 sensitizes Paneth cells in the crypts of the small intestine to necrotic cell death.

TNF-α-stimulated death receptor signalling has been described to promote necrosis in a number of different target cell types, especially when apoptosis was blocked using caspase inhibitors[12,13]. We therefore reasoned that in the absence of caspase-8, TNF-α signalling might lead to excessive crypt cell death. To test this hypothesis, we intravenously administered TNF-α to *Casp8*$^{\Delta IEC}$ mice using a dose that is not lethal

to normal mice. Whereas all control mice were still alive after 5 h, *Casp8*$^{\Delta IEC}$ mice showed significantly more pronounced hypothermia and very high lethality (Supplementary Fig. 7a, b). Histological analysis demonstrated villous atrophy and severe destruction of the small bowel of *Casp8*$^{\Delta IEC}$ mice as compared to control littermates and an increased number of dying epithelial cells, as indicated by the pyknotic nuclei seen in the haematoxylin and eosin (H&E) stain of crypts and cells in the crypt lumen (Supplementary Fig. 7c–e). Similar to unchallenged mice, dying crypt cells were negative for active caspase-3 but positive for TUNEL staining (Supplementary Fig. 8a–c), suggesting that in the absence of caspase-8, TNF drives excessive necrosis of epithelial cells.

Recent data from other experimental systems have shown that inhibition of caspase activity in genetic models or by using specific caspase inhibitors can result in an apoptosis-independent type of programmed necrosis called necroptosis[14]. Necroptosis has been shown to be mediated by the kinases RIP1 and RIP3 (refs 15, 16). On induction of necroptosis, RIP3 is recruited to RIP1 to establish a necroptosis-inducing protein complex. RIP3 seems to be essential for the molecular mechanisms driving necroptosis and expression of *Rip3* has been demonstrated to correlate with the sensitivity of cells towards necroptosis[17,18]. Moreover, deletion of *Rip3* has recently been shown to rescue the lethal phenotype of general caspase-8-deficient mice by blocking cell death[19,20]. Notably, expression of *Rip3* messenger RNA, but not *Rip1* (also known as *Ripk1*) mRNA was significantly increased in IECs isolated from unchallenged *Casp8*$^{\Delta IEC}$ mice as compared to controls (Supplementary Fig. 9). Condensed nuclei as observed in the crypts of *Casp8*$^{\Delta IEC}$ mice stained for RIP3 using immunohistochemistry (Fig. 3a and Supplementary Fig. 8e). Moreover, RIP3 was overexpressed in the small intestine of TNF-α-treated *Casp8*$^{\Delta IEC}$ mice when compared to control littermate mice (Fig. 3b and Supplementary Fig. 8d), suggesting that the lack of caspase-8 in the intestinal epithelium might sensitize IECs to RIP-mediated necroptotic cell death. In line with this hypothesis, RIP3 staining was detected especially in cells at the crypt base (Supplementary Fig. 10). Moreover, significant levels of TNF-α were detected in lamina propria cells adjacent to crypt IECs and both *TNF-α* and *Rip3* expression were highest in the terminal ileum.

RIP-mediated necroptosis can be blocked *in vitro* and *in vivo* by using necrostatin-1 (nec-1), an allosteric small-molecule inhibitor of the RIP1 kinase[21]. Thus we reasoned that nec-1 might prevent TNF-α-induced epithelial necroptosis and lethality in *Casp8*$^{\Delta IEC}$ mice. Indeed, *in vitro*, small intestinal organoid cultures from *Casp8*$^{\Delta IEC}$ mice but not from control mice exhibited necrosis within 24 h after addition of TNF-α to the tissue culture. However, when cell cultures were pre-treated with nec-1, organoid necrosis was blocked (Fig. 3c, d). Moreover, pre-treatment with nec-1 significantly reduced TNF-α-induced lethality and small intestinal tissue destruction in *Casp8*$^{\Delta IEC}$ mice (Fig. 3e, f). Collectively, our data indicate that deficient caspase-8 expression renders Paneth cells susceptible to TNF-α-induced necroptosis, highlighting a regulatory role of caspase-8 in antimicrobial defence and in maintaining immune homeostasis in the gut.

Interestingly, defects in Paneth cell function and in the expression of antimicrobial peptides have been described in Crohn's disease patients and accumulating evidence supports a role for Paneth cells in the pathogenesis of this disease[1,7,22]. As anti-TNF-α treatment is successfully used in the therapy of patients with Crohn's disease, we hypothesized that, similar to *Casp8*$^{\Delta IEC}$ mice, human Paneth cells might be susceptible to TNF-α-induced necroptosis. Paneth cell dysfunction has been reported in mice deficient of autophagy genes such as *Atg16l1*, a gene associated with Crohn's disease susceptibility[3]. Moreover, depletion of Paneth cells in the small intestine has been reported in patients with ileal Crohn's disease and patients with ulcerative colitis involving the terminal ileum[23]. Notably, immunohistochemistry of samples derived from the terminal ileum of human patients undergoing endoscopic examination revealed high expression of *RIP3* exclusively in Paneth cells (Fig. 4a), but not in other intestinal epithelial cell types. Importantly, analysis of histological samples from the terminal ileum of control patients and patients with active Crohn's disease showed a significant decrease in the number of Paneth cells and high numbers of dying cells with shrunken eosinophilic cytoplasm (Fig. 4b) at the crypt base, similar to *Casp8*$^{\Delta IEC}$ mice. Electron microscopy of the Paneth cell area in the terminal ileum of patients with Crohn's disease showed increased necrotic cell death, as indicated by abundant organelle swelling, vacuole formation and the lack of blebbing (Fig. 4c, d). Moreover, crypt epithelial cells in areas of acute inflammation usually were TUNEL positive but lacked staining for active caspase-3 (Fig. 4e). Lastly, ileal biopsies from control patients showed Paneth cell loss in the presence of high levels of exogenous TNF-α, an effect that was reversible by co-incubation with nec-1 (Fig. 4f and Supplementary Fig. 11a). Thus, our data indicate that necroptosis of Paneth cells is a feature of Crohn's disease. As it has recently been shown that anti-TNF treatment partially restores the deficient expression of antimicrobial peptides in Crohn's disease patients[24], our data indicate that the high levels of TNF-α present in the lamina propria of the inflamed ileum induce Paneth cell necroptosis and may provide a molecular explanation for the defects in antimicrobial defence observed in these patients.

Our data uncover an unexpected function of caspase-8 in regulating necroptosis of intestinal epithelial cells and in maintaining immune homeostasis in the gut. Caspase-8-deficient mice had no defect in overall gut morphology, demonstrating that cell death independent from the extrinsic apoptosis pathway can regulate intestinal homeostasis. Indeed, studies using electron microscopy have shown various different cell death morphologies in the small intestine including morphological changes usually seen in necrosis, such as cell swelling and a degradation of organelles and membranes[25]. Caspase-8-deficient mice completely lacked Paneth cells, suggesting that these cell types are highly susceptible to necroptosis. Crohn's disease patients frequently show reduced Paneth and goblet cell numbers and reduced expression of Paneth-cell-derived defensins in areas of acute inflammation, suggesting that necroptosis

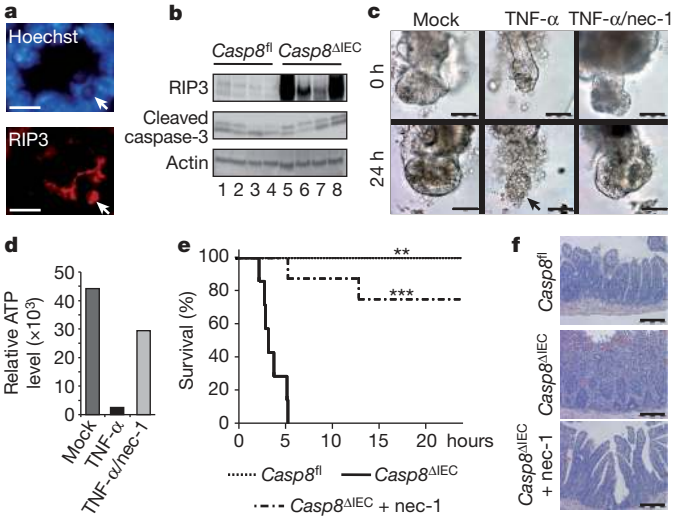

Figure 3 | Inhibition of TNF-α-induced epithelial necroptosis in *Casp8*$^{\Delta IEC}$ mice. **a**, Representative RIP3 staining co-localizing with condensed nuclei (arrows) at the crypt bottom of *Casp8*$^{\Delta IEC}$ mice. Scale bars, 20 μm. **b**, Western blot for RIP3 and cleaved caspase-3 of IEC lysates isolated from TNF-α-treated control and *Casp8*$^{\Delta IEC}$ mice. Actin served as a control. **c**, **d**, Representative microscopic pictures (**c**) and cell viability (**d**) of *Casp8*$^{\Delta IEC}$ organoids treated for 24 h with TNF-α with or without nec-1. Scale bars, 50 μm. Arrow indicates necrotic organoid. **e**, **f**, Survival (**e**) and H&E stained small intestine cross-sections of control ($n = 5$), *Casp8*$^{\Delta IEC}$ (mock pre-treated, $n = 7$) and *Casp8*$^{\Delta IEC}$ (nec-1 pretreated, $n = 8$) mice (**f**) after intravenous injection of TNF-α. All experiments were performed at least 3 times with similar results. Scale bars, 200 μm. $^{**}P < 0.01$, $^{***}P < 0.001$, relative to *Casp8*$^{\Delta IEC}$ without nec-1.

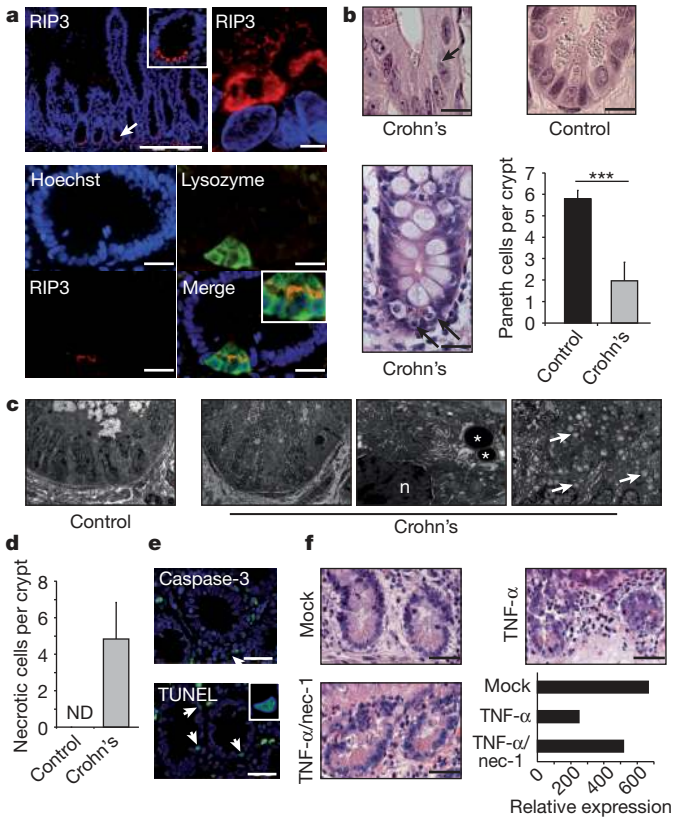

Figure 4 | RIP-mediated necroptosis of Paneth cells in patients with Crohn's disease. a, Representative RIP3 immunostaining of the terminal ileum (healthy patient). Top, RIP3 expression in human Paneth cells (scale bars, 200 μm (left), 5 μm (right)). Bottom, co-localization of lysozyme and RIP3 in Paneth cells (scale bars, 20 μm). Arrow indicates Paneth cells. **b**, H&E staining of crypts in the terminal ileum. Arrows indicate crypt cells with shrunken eosinophilic cytoplasm and pyknotic nuclei (scale bars, 20 μm). Graph shows number of Paneth cells (+ s.d.) per crypt in control patients ($n = 7$) and patients with active Crohn's disease ($n = 4$). $^{***}P < 0.001$. **c**, Electron microscopy of the terminal ileum of control and Crohn's disease patient. Asterisks highlight Paneth cell granules; arrows indicate mitochondrial swelling. n, nucleus. **d**, Number of crypt cells (+ s.d.) showing organelle swelling but regular nuclei as signs of necroptosis. Electron microscope pictures of four patients were analysed. ND, not detectable. **e**, Representative immunofluorescence staining for TUNEL and cleaved caspase-3 in crypts of the terminal ileum of a Crohn's disease patient (scale bars, 50 μm). Arrows indicate Paneth cells. **f**, H&E staining of biopsies from the small intestine of control patients stimulated *in vitro* with either DMSO (mock), TNF-α alone or in combination with nec-1 (scale bars, 50 μm). Graph shows quantitative expression level of the Paneth cell marker lysozyme relative to *HPRT*. Data from one representative experiment out of two is shown.

might be involved in the pathogenesis of human IBD[22]. Indeed, we were able to demonstrate constitutive expression of RIP3—a kinase sensitizing cells to necroptosis[17,18]—in human Paneth cells. Moreover, cells undergoing necroptosis were found at the crypt base in patients with Crohn's disease and Paneth cell death could be inhibited by blocking necroptosis.

Caspase-8 has recently been shown to suppress RIP3–RIP1-kinase-dependent necroptosis following death receptor activation[14,17,18]. This has been highlighted by genetic studies demonstrating that deletion of *Rip3* can rescue the embryonic lethality observed in mice with a general deletion of caspase-8 (refs 19, 20). Thus it is becoming increasingly clear that caspase-8 has an essential function in controlling RIP3-mediated necroptosis. On the molecular level, caspase-8 has been demonstrated to proteolytically cleave and inactivate RIP1 and RIP3, thereby regulating the initiation of necroptosis[20]. So far, to our knowledge, no study has demonstrated caspase-8 as an IBD-linked gene using genetic studies. However, caspase-8 was expressed at relatively low levels in the crypt area of the human terminal ileum and activation of caspase-8 was only seen sporadically along the crypt–villous axis (Supplementary Fig. 11b). Given the low expression of caspase-8 and high expression of RIP3 at the base of crypts, cells residing in this area may be susceptible to necroptosis on stimulation with death receptor ligands such as TNF-α.

TNF-α is an important contributor to the pathogenesis of IBD and treatment with biological drugs targeting TNF-α is effective in patients with Crohn's disease. Interestingly, mice overproducing TNF-α develop transmural intestinal inflammation with granulomas primarily in the terminal ileum, similar to Crohn's disease[26]. TNF-α was a strong promoter of intestinal epithelial necroptosis in our experiments. Because anti-TNF treatment has been shown to restore expression of certain antimicrobial peptides[24] it is tempting to speculate that TNF-α-induced necroptosis of intestinal epithelial cells contributes to the pathogenesis of IBD and that Paneth and goblet cell sensitivity towards TNF-induced necroptosis may be an early event in IBD development. However, it remains to be determined whether Paneth cell necroptosis in Crohn's disease patients is quantitatively sufficient to affect the disease process. Further studies will be needed to decipher the precise regulatory network of death receptors, RIP kinases and caspase-8 at the crypt base and it will be important to elucidate whether genetic, epigenetic or post-translational mechanisms restrict expression or activation of caspase-8 in IBD patients. Here, our data for the first time demonstrate necroptosis in the terminal ileum of patients with Crohn's disease and indicate that regulating necroptosis in the intestinal epithelium is critical for the maintenance of intestinal immune homeostasis. Targeting necroptotic cellular mechanisms emerges as a promising option in treating patients with IBD.

METHODS SUMMARY

Mice carrying a *loxP*-flanked caspase-8 allele (*Casp8*^{fl}) and villin-*Cre* mice were described earlier[27–29]. IEC-specific caspase-8 knockout mice were generated by breeding *Casp8*^{fl} mice to villin-*Cre* or villin-*CreERT2* mice. Experimental colitis was induced with 1–1.5% dextrane sodium sulphate (DSS; MP Biomedicals) in the drinking water for 5–10 days. Colitis development was monitored by analysis of weight, rectal bleeding and colonoscopy as previously described[30]. In some experiments, mice were injected intravenously with TNF-α (200 ng g^{-1} body weight; Immunotools) plus or minus nec-1 (1.65 μg g^{-1} body weight; Enzo). Histopathological analysis was performed on formalin-fixed paraffin-embedded tissue after H&E staining. Immunofluorescence of cryosections was performed using the TSA-Kit as recommended by the manufacturer (PerkinElmer). For electron microscopy, glutaraldehyde-fixed material was used. Ultrathin sections were cut and analysed using a Zeiss EM 906. Paraffin-embedded patient specimens were obtained from the Institute of Pathology and endoscopic biopsies were collected in the Department of Medicine 1 (Erlangen University). The collection of samples was approved by the local ethical committee and each patient gave written informed consent. For organoid culture, intestinal crypts were isolated from mice and cultured as previously described[11]. Organoid growth was monitored by light microscopy. IECs were isolated as previously described[5]. For gene-chip experiments, total RNA of IECs was isolated using the RNeasy Mini Kit (Qiagen) and hybridized to the Affymetrix mouse 430 2.0 chip (Affymetrix). GO-based analyses were performed using the online tool Database for Annotation, Visualization and Integrated Discovery (DAVID). Caspase-3/-7 activity was measured using the Caspase-Glo3/7 Assay (Promega) according to the manufacturer's instructions.

Full Methods and any associated references are available in the online version of the paper at www.nature.com/nature.

Received 2 February; accepted 2 August 2011.

1. Strober, W., Fuss, I. & Mannon, P. The fundamental basis of inflammatory bowel disease. *J. Clin. Invest.* **117,** 514–521 (2007).
2. Artis, D. Epithelial-cell recognition of commensal bacteria and maintenance of immune homeostasis in the gut. *Nature Rev. Immunol.* **8,** 411–420 (2008).
3. Kaser, A., Zeissig, S. & Blumberg, R. S. Inflammatory bowel disease. *Annu. Rev. Immunol.* **28,** 573–621 (2010).
4. Hall, P. A. *et al.* Regulation of cell number in the mammalian gastrointestinal tract: the importance of apoptosis. *J. Cell Sci.* **107,** 3569–3577 (1994).
5. Nenci, A. *et al.* Epithelial NEMO links innate immunity to chronic intestinal inflammation. *Nature* **446,** 557–561 (2007).

6. Sanders, D. S. Mucosal integrity and barrier function in the pathogenesis of early lesions in Crohn's disease. *J. Clin. Pathol.* **58,** 568–572 (2005).
7. Elphick, D. A. & Mahida, Y. R. Paneth cells: their role in innate immunity and inflammatory disease. *Gut* **54,** 1802–1809 (2005).
8. Maelfait, J. & Beyaert, R. Non-apoptotic functions of caspase-8. *Biochem. Pharmacol.* **76,** 1365–1373 (2008).
9. Valmiki, M. G. & Ramos, J. W. Death effector domain-containing proteins. *Cell. Mol. Life Sci.* **66,** 814–830 (2009).
10. Mielgo, A. *et al.* The death effector domains of caspase-8 induce terminal differentiation. *PLoS ONE* **4,** e7879 (2009).
11. Sato, T. *et al.* Single Lgr5 stem cells build crypt-villus structures *in vitro* without a mesenchymal niche. *Nature* **459,** 262–265 (2009).
12. Holler, N. *et al.* Fas triggers an alternative, caspase-8-independent cell death pathway using the kinase RIP as effector molecule. *Nature Immunol.* **1,** 489–495 (2000).
13. Vercammen, D. *et al.* Tumour necrosis factor-induced necrosis versus anti-Fas-induced apoptosis in L929 cells. *Cytokine* **9,** 801–808 (1997).
14. Vandenabeele, P. *et al.* Molecular mechanisms of necroptosis: an ordered cellular explosion. *Nature Rev. Mol. Cell Biol.* **11,** 700–714 (2010).
15. Cho, Y. S. *et al.* Phosphorylation-driven assembly of the RIP1–RIP3 complex regulates programmed necrosis and virus-induced inflammation. *Cell* **137,** 1112–1123 (2009).
16. Declercq, W., Vanden Berghe, T. & Vandenabeele, P. RIP kinases at the crossroads of cell death and survival. *Cell* **138,** 229–232 (2009).
17. He, S. *et al.* Receptor interacting protein kinase-3 determines cellular necrotic response to TNF-α. *Cell* **137,** 1100–1111 (2009).
18. Zhang, D. W. *et al.* RIP3, an energy metabolism regulator that switches TNF-induced cell death from apoptosis to necrosis. *Science* **325,** 332–336 (2009).
19. Kaiser, W. J. *et al.* RIP3 mediates the embryonic lethality of caspase-8-deficient mice. *Nature* **471,** 368–372 (2011).
20. Oberst, A. *et al.* Catalytic activity of the caspase-8–$FLIP_L$ complex inhibits RIPK3-dependent necrosis. *Nature* **471,** 363–367 (2011).
21. Degterev, A. *et al.* Identification of RIP1 kinase as a specific cellular target of necrostatins. *Nature Chem. Biol.* **4,** 313–321 (2008).
22. Wehkamp, J. *et al.* Barrier dysfunction due to distinct defensin deficiencies in small intestinal and colonic Crohn's disease. *Mucosal Immunol.* **1** (Suppl. 1), S67–S74 (2008).
23. Lewin, K. The Paneth cell in disease. *Gut* **10,** 804–811 (1969).
24. Arijs, I. *et al.* Mucosal gene expression of antimicrobial peptides in inflammatory bowel disease before and after first infliximab treatment. *PLoS ONE* **4,** e7984 (2009).
25. Mayhew, T. M. *et al.* Epithelial integrity, cell death and cell loss in mammalian small intestine. *Histol. Histopathol.* **14,** 257–267 (1999).
26. Kontoyiannis, D. *et al.* Impaired on/off regulation of TNF biosynthesis in mice lacking TNF AU-rich elements: implications for joint and gut-associated immunopathologies. *Immunity* **10,** 387–398 (1999).
27. Beisner, D. R. *et al.* Cutting edge: innate immunity conferred by B cells is regulated by caspase-8. *J. Immunol.* **175,** 3469–3473 (2005).
28. Madison, B. B. *et al. cis* elements of the villin gene control expression in restricted domains of the vertical (crypt) and horizontal (duodenum, cecum) axes of the intestine. *J. Biol. Chem.* **277,** 33275–33283 (2002).
29. El Marjou, F. *et al.* Tissue-specific and inducible Cre-mediated recombination in the gut epithelium. *Genesis* **39,** 186–193 (2004).
30. Becker, C. *et al. In vivo* imaging of colitis and colon cancer development in mice using high resolution chromoendoscopy. *Gut* **54,** 950–954 (2005).

Supplementary Information is linked to the online version of the paper at www.nature.com/nature.

Acknowledgements The research leading to these results has received funding from the Interdisciplinary Center for Clinical Research (IZKF) of the University Erlangen-Nuremberg and the European Community's 7th Framework Program (FP7/2007-2013) under grant agreement no. 202230, acronym GENINCA. E.M. received funding from the Welcome Trust (WT087768MA) and S.M.H. was supported by NIH grant AI037988. The authors thank A. Watson for critical reading of the manuscript, A. Nikolaev, S. Wallmüller, V. Buchert and M. Klewer for technical assistance and J. Mudter, R. Atreya and C. Neufert for sampling biopsies.

Author Contributions C.G., K.A., M.F.N. and C.B. designed the research. C.G., E.M., N.W., B.W., H.N., M.W. and S.T. performed the experiments. S.M.H. provided material that made the study possible. C.G., K.A. and C.B. analysed the data and wrote the paper.

Author Information Chip data were deposited at the NCBI Gene Expression Omnibus under the series accession number GSE30873 (http://www.ncbi.nlm.nih.gov/geo/query/acc.cgi?acc=GSE30873). Reprints and permissions information is available at www.nature.com/reprints. The authors declare no competing financial interests. Readers are welcome to comment on the online version of this article at www.nature.com/nature. Correspondence and requests for materials should be addressed to C.B. (christoph.becker@uk-erlangen.de).

METHODS

Mice. Mice carrying a *loxP*-flanked caspase-8 allele (*Casp8*^{fl}) and villin-*Cre* mice were described earlier[27–29]. Intestinal-epithelium-specific caspase-8 knockout mice were generated by breeding floxed caspase-8 mice to either villin-*Cre* or villin-*CreERT2* mice. For the induction of the CreERT2 line (villin-*CreERT2*× *Casp8*^{fl}), tamoxifen (50 mg ml^{-1} ethanol; Sigma) was emulsified in sunflower oil at a concentration of 5 mg ml^{-1}. Mice were injected daily intraperitoneally with 200 µl of tamoxifen. In all experiments, littermates carrying the *loxP*-flanked alleles but not expressing Cre recombinase were used as controls. Cre-mediated recombination was genotyped by PCR on tail DNA. Experimental colitis was induced by treating mice with 1–1.5% dextrane sodium sulphate (DSS; MP Biomedicals) in the drinking water for 5–10 days. DSS was exchanged every other day. In some experiments, mice were injected intravenously with rm-TNF (200 ng g^{-1} body weight; Immunotools) plus or minus nec-1 (1.65 µg g^{-1} body weight; Enzo). Mice were examined by measuring body temperature, weight loss and monitoring development of diarrhoea. Colitis development was monitored by analysis of rectal bleeding and high-resolution mouse video endoscopy as previously described[29]. Mice were anaesthetized with 2–2.5% isoflurane in oxygen during endoscopy. Mice were routinely screened for pathogens according to FELASA guidelines. Animal protocols were approved by the Institutional Animal Care and Use Committee of the University of Erlangen.

Human samples. Paraffin-embedded specimens from the terminal ileum of control patients and patients with active Crohn's disease were obtained from the Institute of Pathology of the University Clinic Erlangen. The specimens had been taken from routine diagnostic samples and patient data had been made anonymous. Electron microscopy and tissue culture experiments were performed with endoscopic biopsy specimens collected in the endoscopy ward of the Department of Medicine 1. The collection of samples was approved by the local ethical committee and the institutional review board of the University of Erlangen-Nuremberg and each patient gave written informed consent.

Histology, immunohistochemistry and electron microscopy. Histopathological analysis was performed on formalin-fixed paraffin-embedded tissue after H&E staining. Immunofluorescence of cryosections was performed using the TSA Cy3 system as recommended by the manufacturer (PerkinElmer). Fluorescence microscopy (Olympus) and confocal microscopy (Leica TCS SP5) was used for analysis. The following primary antibodies were used: CD4 (BD Bioscience), myeloperoxidase (Zymed Labs), F4/80 (MD Bioscience), caspase-8 (Sigma), cleaved caspase-8, cleaved caspase-3 (Cell Signaling Technology), lysozyme, chromogranin-A (Invitrogen), human RIP3 (Abcam), mouse RIP3 (AbD Serotec) and TNF-α (Pharmingen). Slides were then incubated with biotinylated secondary antibodies (Dianova). The nuclei were counterstained with Hoechst 3342 (Invitrogen). Cell death was analysed using CaspACE FITC-VAD-FMK (Promega) for early apoptosis and the *in situ* cell death detection kit (Roche) for TUNEL. For electron microscopy, glutaraldehyde-fixed material was used. After embedding in Epon Araldite, ultrathin sections were cut and analysed using a Zeiss EM 906.

Crypt isolation and organoid culture. Organ culture of freshly isolated human small intestinal biopsies was performed in RPMI medium (Gibco). For organoid culture, crypts were isolated from the small intestine of mice and cultured for a minimum of 7 days as previously described[11]. In brief, crypts were isolated by incubating pieces of small intestine in isolation buffer (phosphate buffered saline without calcium and magnesium (PBS0), 2 mM EDTA). Crypts were then transferred into matrigel (BD Bioscience) in 48-well plates and 350 µl culture medium (advanced DMEM/F12 (Invitrogen), containing HEPES (10 mM; PAA), GlutaMax (2 mM; Invitrogen), penicillin (100 U ml^{-1}; Gibco), streptomycin (100 µg ml^{-1}; Gibco), murine EGF (50 ng ml^{-1}; Immunotools), recombinant human R-spondin (1 µg ml^{-1}; R&D Systems), N2 Supplement 1× (Invitrogen), B27 Supplement 1× (Invitrogen), 1 mM N-acetylcystein (Sigma-Aldrich) and recombinant murine Noggin (100 ng ml^{-1}; Peprotech)). Organoid growth was monitored by light microscopy. In some experiments, human biopsies or organoids were treated with recombinant mouse TNF-α (25 ng ml^{-1}; Immunotools), recombinant human TNF-α (50 ng ml^{-1}; Immunotools), nec-1 (30 µM; Enzo) or caspase-8 inhibitor (50 µM; Santa Cruz). Cell viability of organoids was analysed indirectly by quantification of relative ATP level with the CellTiter-Glo assay from Promega according to the manufacturer's instructions. Luminescence was measured on the microplate reader infinite M200 (Tecan).

IEC isolation and immunoblotting. IECs were isolated in an EDTA separation solution as previously described[5]. Protein extracts were prepared using the mammalian protein extraction reagent (Thermo Scientific) supplemented with protease and phosphatase inhibitor tablets (Roche). Protein extracts were separated by SDS–PAGE (10%) and transferred to nitrocellulose transfer membranes (Whatman). Membranes were probed with the following primary antibodies: cleaved caspase-8, cleaved caspase-3, cleaved caspase-9 (Cell Signaling), RIP3 (Enzo), actin (Santa Cruz Biotechnology) and secondary HRP-linked anti-rabbit antibody (Cell Signaling).

Gene expression analyses. Total RNA was extracted from gut tissue or isolated IECs using an RNA isolation kit (Nucleo Spin RNA II, Macherey Nagel). cDNA was synthesized by reverse transcription (iScript cDNA Synthesis Kit, Bio Rad) and analysed by real-time PCR with SsoFast EvaGreen (Bio-Rad) reagent and QuantiTect Primer assays (Qiagen). Experiments were normalized to the level of the housekeeping gene *HPRT*. For gene-chip experiments total RNA of IECs from three control and three *Casp8*$^{\Delta IEC}$ mice was isolated using the RNeasy Mini Kit (Qiagen) and were performed by the Erlangen University core facility using the Affymetrix mouse 430 2.0 chip (Affymetrix). For multiple gene array testing including differential expression analysis the software package FlexArray (http://genomequebec.mcgill.ca/FlexArray) was used. GO-based analyses were performed using the online tool Database for Annotation, Visualization and Integrated Discovery (DAVID).

Caspase activity. Primary isolated intestinal epithelial cells were cultured with RPMI (Gibco), supplemented with 10% FCS (PAA), penicillin (100 U ml^{-1}; Gibco), streptomycin (100 µg ml^{-1}; Gibco) in fibronectin (BD Bioscience) coated 48-well plates and caspase-3/-7 activity was measured using the Caspase-Glo3/7 Assay from Promega according to the manufacturer's instructions. Luminescence was measured on the microplate reader infinite M200 (Tecan).

Statistical analysis. Data were analysed by Student's *t*-test using Microsoft Excel. $^{*}P < 0.05$, $^{**}P < 0.01$, $^{***}P < 0.001$.